Real-time PCR was performed on an ABI Prism 7700 Sequence Detection System (Applied Biosystems). The miR-122 expression in the samples was quantified by the relative standard curve method using a control sample (histopathologically normal liver sample from a patient with metastatic liver tumour) and normalized by RNU6B expression. After normalization, the expression values were calculated relative to the control sample (the liver sample or serum sample from the patient with metastatic liver tumour).

Quantification of serum and hepatic HCV load

Quantification of pre-operative serum HCV RNA load (Log IU/mL) and/or the pre-operative HCV genotyping was performed by SRL Inc. Fukuoka Laboratory (Fukuoka, Japan) using a COBAS Amplicor HCV Monitor version 2.0 or COBAS Taqman® HCV assays (Roche Diagnostics, Mannheim, Germany). Hepatic HCV RNA load (log copies/μg of total RNA) in the total RNA was also quantified by SRL Inc. Fukuoka Laboratory using the qRT-PCR method, as described previously (17). Total RNA (1 μg) isolated from the liver samples, as above, was used to quantify hepatic HCV RNA levels using a qRT-PCR assay.

Histopathological examination of liver samples

Histopathological examination of the non-cancerous livers was performed according to the METAVIR scoring system (18). The differentiation of HCC was graded according to the Edmondson and Steiner criteria (grade 1, well differentiated; grade 2, moderately differentiated; and grade 3, poorly differentiated) (19). The pathological stage of HCCs was determined according to the tumour-node-metastasis staging criteria of the International Union Against Cancer and the American Joint Committee on Cancer (20). The histopathological characteristics of the patients are also shown in Table 1.

Statistical analyses

The miR-122 expression is expressed as the median (range) and is presented as box plots. Other continuous variables, including HCV load, are expressed as means ± standard deviation, and presented as scatter plots. Pearson's correlation coefficients were calculated to determine correlations between the serum and hepatic HCV loads. Spearman's rank correlation was used to determine the correlation between miR-122 expression and HCV load, hepatic function (Child–Pugh grades), serum transaminase levels, inflammatory activity, fibrosis stage and serum miR-122 level. The association between miR-122 expression and HCV load was also evaluated for both genotypes (genotypes 1 and 2). Accordingly, it should be considered that the ratio of hepatocytes to other cell types in the specimens could relatively decrease because of the growth of cells other than hepatocytes, such as lymphocytes, macrophages, fibroblasts, stellate cells and myofibroblasts, as liver damage progresses. Thus, it is possible that the expression of liver specific miR-122 may be underestimated in severely damaged liver samples. To eliminate a possible effect of non-hepatocyte cells, a stratified analysis was also performed according to grades of inflammation activity (A0/1, A2, A3) and fibrosis stage (F0/1, F2/3, F4). The Mann–Whitney *U*-test was used to determine differences in miR-122 expression between two groups. The Breslow–Gehan–Wilcoxon test was used to evaluate differences in miR-122 expression between the HCCs and the paired non-cancerous livers. *P*-values < 0.05 were considered to be statistically significant. All statistical analyses were performed using STATVIEW® 5.0 software (Abacus Concepts, Berkeley, CA, USA).

Results

Serum and hepatic hepatitis C virus load

Overall, 185 patients were seropositive for the HCV antibody. Of these, 151 patients were positive for serum HCV RNA and 31 patients were negative for serum HCV RNA (Table 1). In the 151 seropositive patients, the mean serum HCV load was 5.6 ± 0.7 log IU/ml, the mean hepatic HCV load was 6.0 ± 1.0 log copies/μg of total RNA; the hepatic HCV load in two cases was below the measurable limit (2.3 log copies/μg of total RNA). The serum HCV load was positively correlated with the hepatic HCV load ($r = 0.531$, $P < 0.0001$; Fig. 1A). The strength of the correlation was similar to that in a previous report ($r = 0.689$, $P = 0.004$, $n = 15$) (21).

Association between hepatic microRNA-122 expression and hepatitis C virus load

The median hepatic miR-122 expression in all non-cancerous cases was 0.34 (range, 0.02–3.36; $n = 204$), relative to the control sample by qRT-PCR. The median non-cancerous hepatic miR-122 expression in the HCV-infected group and control group was 0.32 (range, 0.02–3.36; $n = 185$) and 0.61 (range, 0.31–2.50; $n = 19$) respectively. We analysed the correlation between the hepatic miR-122 expression and the serum and hepatic HCV loads in non-cancerous samples. The expression of hepatic miR-122 in non-cancerous liver tissue was weakly but positively correlated with the serum HCV load ($\rho = 0.19$, $P < 0.05$; Fig. 1B), but not with the hepatic HCV load ($\rho = -0.14$, $P = 0.08$; Fig. 1C). Furthermore, the expression of hepatic miR-122 in non-cancerous serum HCV-negative patients ($n = 31$) was significantly higher than that in the serum HCV-positive patients ($n = 151$) ($P < 0.0001$) and similar to that in the control cases (Fig. 1D). The association between miR-122 expression and HCV load was analysed for both genotypes 1 and 2. In patients with genotype 1, hepatic miR-122 expression was not correlated with the serum HCV load ($\rho = 0.14$, $P = 0.16$; Fig. 2A) and was weakly and

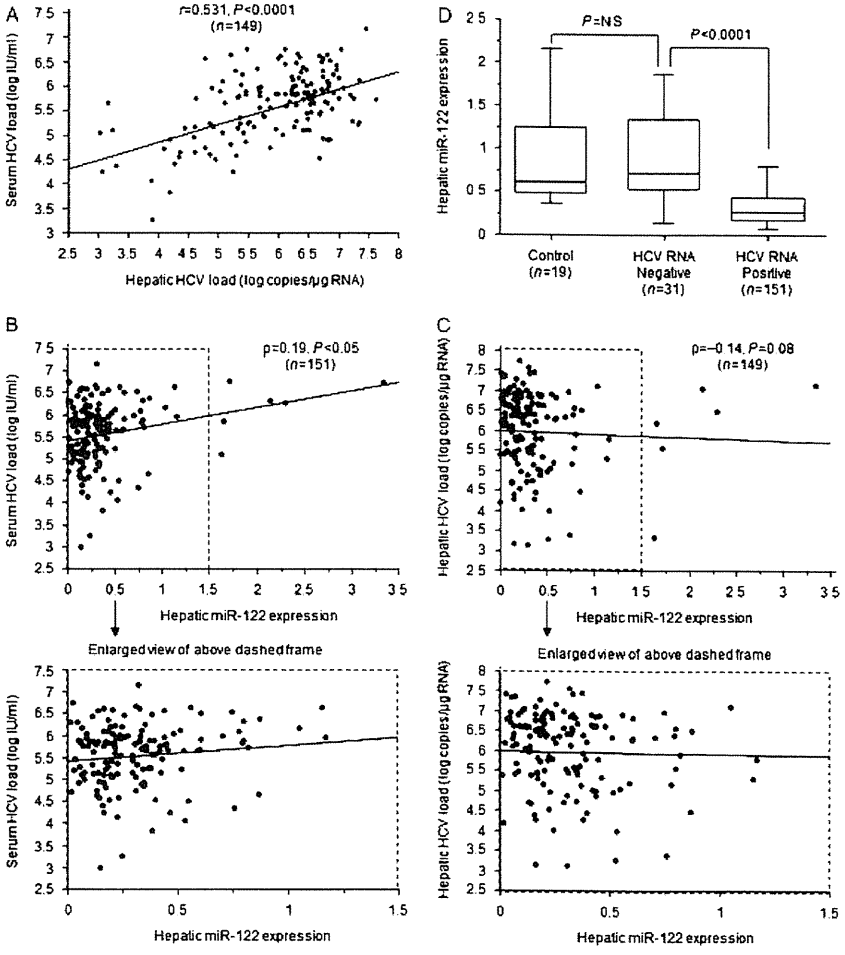

Fig. 1. The association between hepatic microRNA-122 (miR-122) expression of hepatitis C virus (HCV)-infected liver and HCV load. MiR-122 expression was quantified relative to the control sample (histopathologically normal liver with metastatic liver tumour) by quantitative reverse-transcription polymerase chain reaction. The serum HCV load was positively correlated with the hepatic HCV load ($r = 0.531$, $P < 0.0001$) (A). Hepatic miR-122 expression was weakly and positively correlated with the serum HCV load ($\rho = 0.19$, $P < 0.05$) (B). Hepatic miR-122 expression was not correlated with the hepatic HCV load ($\rho = -0.14$, $P = 0.08$) (C). Hepatic miR-122 expression in cases seronegative for HCV RNA was significantly higher than that in cases seropositive for HCV RNA ($P < 0.0001$) and similar to that in the control cases (D). NS, not significant.

inversely correlated with the hepatic HCV load ($\rho = -0.21$, $P < 0.05$; Fig. 2B). In patients with genotype 2, hepatic miR-122 expression was not correlated with the serum or hepatic HCV loads ($\rho = 0.03$, $P = 0.89$; $\rho = 0.17$, $P = 0.40$ respectively; Fig. 2C and D).

Stratified analyses to evaluate the correlation between microRNA-122 expression and hepatitis C virus load

In the stratified analyses, hepatic miR-122 was not positively correlated with hepatic HCV load. In A3 cases, there was a significant negative correlation ($\rho = -0.54$, $P < 0.05$; Fig. 3A–F). The expression of hepatic miR-122 in non-cancerous serum HCV-negative patients was significantly higher than that in serum HCV-positive patients in the A0/1, A2, F0/1 and F2/3 cases. However, there was no difference in the stratified analyses in the A3 and F4 cases, in which the number of cases in each group was small or disproportionate (Fig. 4A–F).

Functional and histopathological liver damage

Because miR-122 is abundantly expressed miRNA in the liver, we analysed the hepatic miR-122 expression according to the hepatic function and histopathological liver damage. The expression of miR-122 was inversely correlated with the functional liver damage (Child–Pugh grade) ($\rho = -0.61$, $P < 0.0001$; Fig. 5A), serum aspartate aminotransferase level ($\rho = -0.52$, $P < 0.0001$; Fig. 5B), serum alanine aminotransferase level ($\rho = -0.26$,

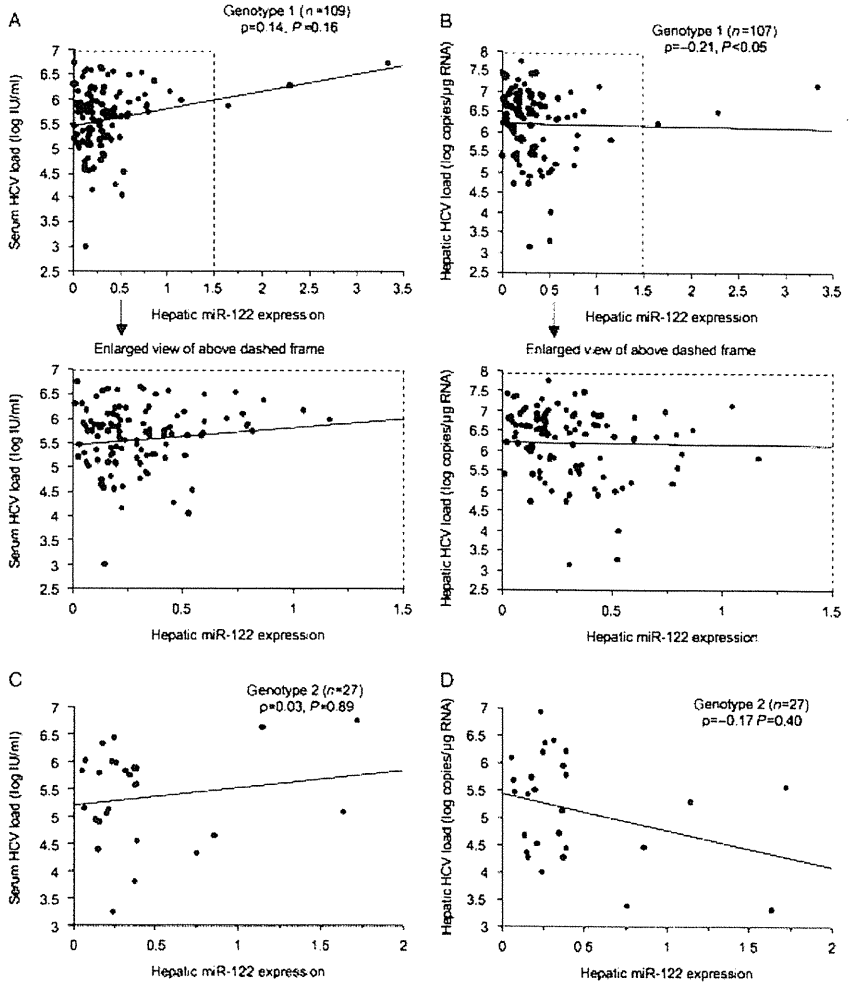

Fig. 2. The association between microRNA-122 (miR-122) expression and hepatitis C virus (HCV) load in genotypes 1 and 2. In genotype 1, miR-122 expression was not correlated with serum HCV load ($\rho = 0.14$, $P = 0.16$) (A), but was weakly and negatively correlated with hepatic HCV load ($\rho = -0.21$, $P < 0.05$) (B). In genotype 2, miR-122 expression was not correlated with serum or hepatic HCV load ($\rho = 0.03$, $P = 0.89$; $\rho = -0.17$, $P = 0.40$ respectively) (C, D).

$P < 0.0005$; Fig. 5C), histopathological inflammation activity grade ($\rho = -0.44$, $P < 0.0001$; Fig. 5D) and fibrosis stage ($\rho = -0.55$, $P < 0.0001$; Fig. 5E). The median serum miR-122 level was 0.537 (range, 0.077–3.270; $n = 40$), relative to the control serum sample by qRT-PCR. The hepatic miR-122 expression was positively correlated with the serum miR-122 level ($\rho = 0.37$, $P < 0.05$; Fig. 5F). The correlation between miR-122 expression and functional liver damage was also confirmed in the stratified analyses for inflammation activity grade A0/1 and A2, and fibrosis stage F4. There was no significant correlation in the stratified analyses in the A3, F0/1 and F2/3 cases, in which the number of cases in each group was small or disproportionate (Fig. 6A–F).

MicroRNA-122 expression in hepatic cancer

In the present study, 139 nodules of hepatic cancers were assayed and miR-122 expression was compared between the hepatic cancer samples and the paired non-cancerous liver samples. MiR-122 expression in the cancer samples was significantly lower than that of the paired non-cancerous livers ($P < 0.05$). The expression of miR-122 in the paired non-cancerous liver samples was significantly lower than that in the control normal liver samples ($P < 0.001$; Fig. 7A). The miR-122 expression in cancerous poorly differentiated hepatic cancer was significantly lower than that in moderately differentiated hepatic cancer ($P < 0.0001$; Fig. 7B). The expression of miR-122 in the cancerous T2 and T3 cases was significantly lower

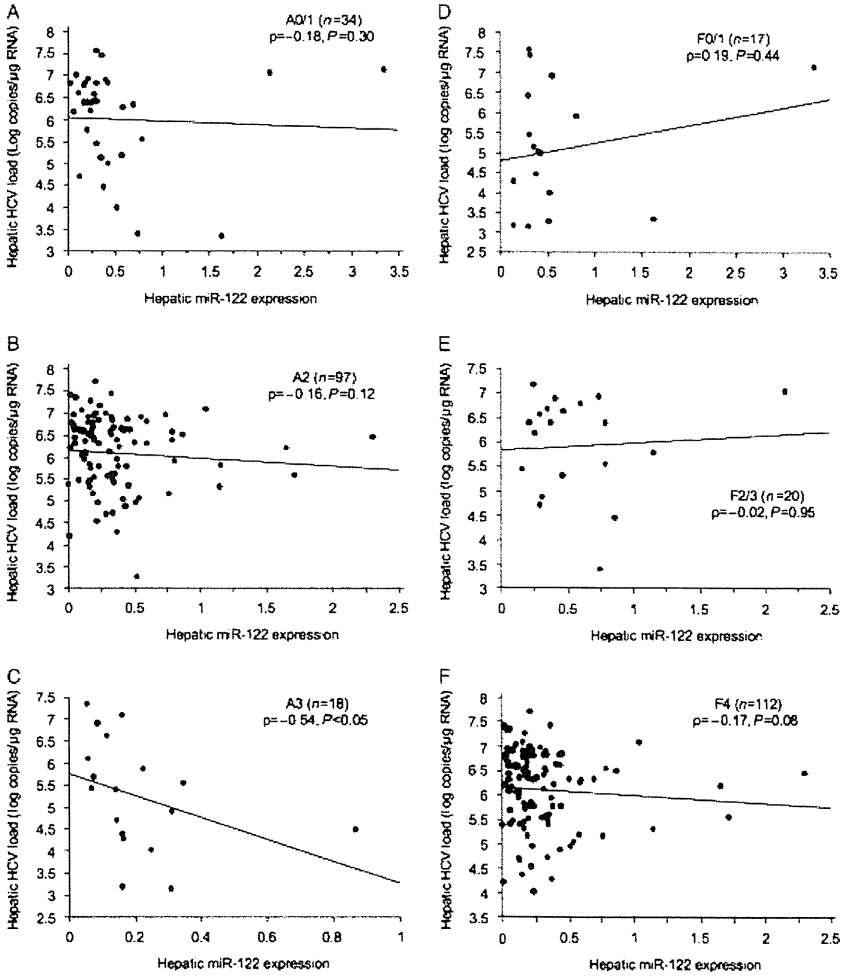

Fig. 3. Stratified analyses to confirm the association between microRNA-122 (miR-122) and hepatic hepatitis C virus (HCV) load. Hepatic miR-122 expression was not correlated with hepatic HCV load in the stratified analyses in the A0/1 or A2 grades of inflammatory activity or in any stage of fibrosis (F0/1, F2/3, F4) (A, B, D–F), but was significantly negatively correlated with hepatic HCV load in inflammatory activity grade A3 ($\rho = -0.54$, $P < 0.05$) (C).

than that in the T1 cases ($P < 0.0001$ and $P < 0.01$ respectively; Fig. 7C).

Discussion

The present study provided a surprising but consistent finding that hepatic miR-122 expression is not correlated with the hepatic HCV load, based on a large number of cases and stratified analyses. A liver-specific miRNA, miR-122 has been reported to facilitate the replication of HCV *in vitro* (9–14). These *in vitro* reports have increased the interest regarding the effect of miR-122 on hepatitis C, and the expectation that inhibition of hepatic miR-122 may contribute to novel molecular-targeted therapy of hepatitis C (9–15). However, the association between miR-122 and HCV in humans is still unclear. Recently, Sarasin-Filipowicz *et al.* (16) reported an analysis of liver biopsies from 42 subjects seropositive for HCV RNA undergoing IFN therapy, and revealed no correlation between miR-122 expression and viral load. Their study provided a perspective on the role of miRNAs in HCV infection. However, the number ($n = 42$) was small and no correlation was observed in these cases with broad range of inflammatory activity grades and fibrosis stages, which was possibly because of a relative decrease in the number of hepatocytes. To clarify the clinical role of miR-122 in patients with HCV, we quantified the hepatic miR-122 expression in a large number of HCV-infected patients and performed detailed analyses with stratification for liver damage.

As a result, hepatic miR-122 expression was not correlated with the hepatic HCV load throughout the

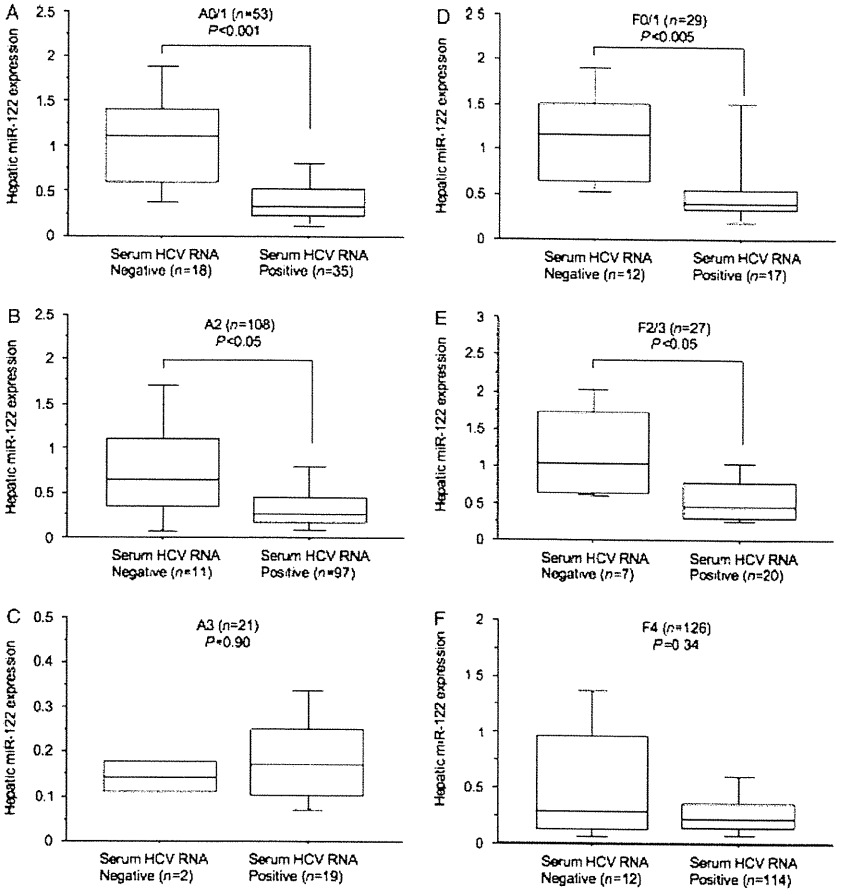

Fig. 4. Stratified analyses to evaluate microRNA-122 (miR-122) expression in cases seronegative for hepatitis C virus (HCV) RNA and cases seropositive for HCV RNA according to grade of inflammatory activity and stage of fibrosis. The hepatic miR-122 expression in cases seronegative for HCV RNA was significantly higher than that in cases seropositive for HCV RNA in the analyses of A0/1, A2, F0/1 and F2/3 cases (A, B, D, E). There was no significant difference in the analysis of the A3 and F4 cases (C, F).

wide range of miR-122 expression level and viral load. Furthermore, hepatic miR-122 expression in cases seronegative for HCV RNA was higher than that in cases seropositive for HCV RNA and similar to that in the healthy control cases, which is a novel finding. Then, the patients without detectable HCV-PCR can be considered to be cured from HCV and can be classified as being similar to healthy control patients in terms of the similar miR-122 expression. Hepatic miR-122 expression was significantly correlated with the serum HCV load, but the correlation was very weak ($\rho = 0.19$, $P < 0.05$). Nevertheless, the absence of a *direct* correlation between *hepatic* miR-122 expression and *hepatic* HCV load should be emphasized more than the *indirect* weak correlation between *hepatic* miR-122 expression and *serum* HCV load. Although the miR-122 targeting regions in the HCV 5′-UTR are highly conserved between the six HCV genotypes (9, 10), we analysed the association between miR-122 expression and HCV load in genotypes 1 and 2. However, miR-122 expression was not positively correlated with either serum or hepatic HCV load in either of these genotypes. Our analysis is based on the large number of cases ($n = 185$), which included 151 cases seropositive for HCV RNA and 31 cases seronegative for HCV RNA. Furthermore, the absence of a correlation between hepatic miR-122 and hepatic HCV load was confirmed in each grade of inflammation activity and stage of fibrosis. This stratified analysis accounted for possible effects of injury-induced growth of cells other than hepatocytes, which leads to a relative decrease in the number of hepatocytes, and was strongly supportive of our hypothesis. Accordingly, our study is more robust because of the larger number of subjects and the use of stratified analyses.

Why miR-122 expression is not correlated with hepatic HCV load is currently not well understood. There are at least two possibilities. Firstly, it may be associated with the existence of many other factors promoting HCV

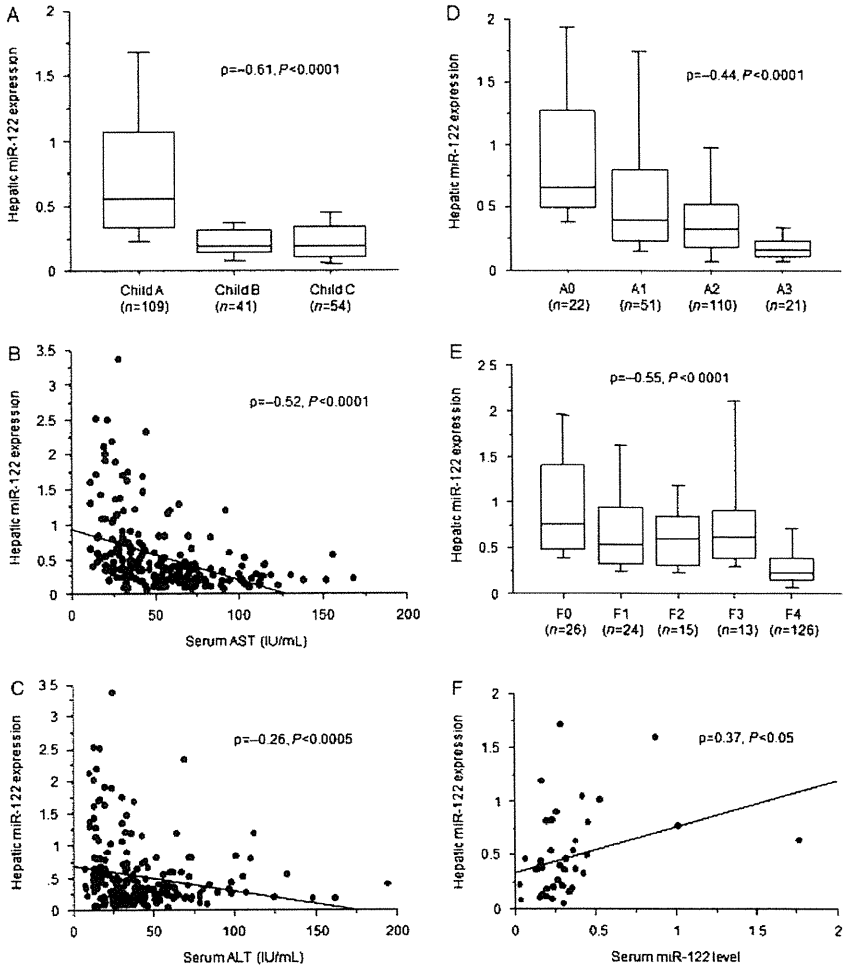

Fig. 5. The expression of microRNA-122 (miR-122) is inversely correlated with liver damage. The level of hepatic miR-122 expression was inversely correlated with the severity of functional liver damage ($\rho = -0.61$, $P < 0.0001$) (A), serum aspartate aminotransferase (AST) level ($\rho = -0.52$, $P < 0.0001$) (B), serum alanine aminotransferase (ALT) level ($\rho = -0.26$, $P < 0.0005$) (C), grade of inflammatory activity ($\rho = -0.44$, $P < 0.0001$) (D), and stage of fibrosis ($\rho = -0.55$, $P < 0.0001$) (E). The hepatic miR-122 expression was positively correlated with the serum miR-122 level ($\rho = 0.37$, $P < 0.05$) (F).

replication. Secondly, lower levels of miR-122 in HCV-infected liver may still be sufficient to support HCV replication. Many factors have been reported to promote HCV replication and production, including the human homologue of the 33 kDa vesicle-associated membrane protein-associated protein (22), vesicle-associated membrane protein-associated protein-B (23), cyclophilin B (24), FK506-binding protein 8, heat shock protein 90 (25), FBL2 (26), fatty acids synthase (27), geranylgeranylation, fatty acids (28) and lipid droplets (29). In the present study, hepatic miR-122 expression was decreased as the functional and histopathological liver injury became more severe. In humans, it was conceivable that HCV will have difficulty replicating during liver injury because HCV replication is dependent on miR-122, which is decreased as liver injury progresses. Therefore, it is possible that HCV replication in injured liver is dependent on factors other than miR-122. In that case, simple repression of miR-122 would be ineffective for the treatment of hepatitis C in humans, and any therapies for HCV based on miR-122 would need to consider a combination with therapies targeting these promoting factors or existing therapies such as IFN therapy. On the other hand, lower levels of miR-122 in HCV-infected liver may still be sufficient to support HCV replication. If so, anti-miR-122 monotherapy for HCV must be destructively strong enough to deplete hepatic miR-122 or at least overcome the physiological wide range of miR-122 expression (range, 0.02–3.36; maximum–minimum ratio, 168 in the present study). Although our results do

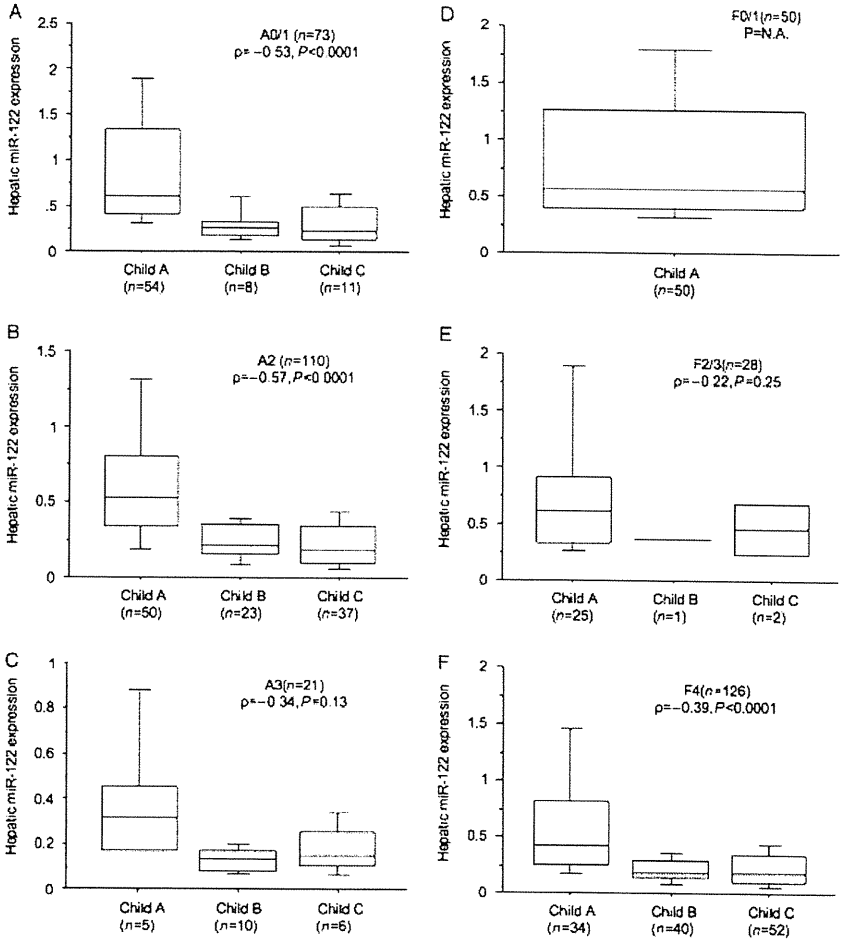

Fig. 6. Stratified analyses to confirm the inverse correlation between microRNA-122 (miR-122) expression and functional liver damage. The inverse correlation was confirmed in the stratified analyses of A0/1, A2 and F4 cases ($\rho = -0.53$, $P < 0.0001$; $\rho = -0.57$, $P < 0.0001$; $\rho = -0.39$, $P < 0.0001$ respectively) (A, B, F). There was no significant correlation in A3, F0/1, and F2/3 cases (C–E).

not preclude the potential of miR-122 as a molecular target for HCV therapy, it would be realistic and practical to combine anti-miR-122 therapy with other therapies for HCV. Recently, Lanford *et al.* (30) reported that antagomir-122 treatment leads to suppression of viraemia in chronically HCV-infected chimpanzees. Absence of viraemia was not observed in their report. Further studies are needed to experimentally and clinically confirm the effect of anti-miR-122 therapy on HCV. The regulatory mechanisms of HCV replication by miRNA should be studied. The effects of miR-122 depend on the context and location of its binding sites in HCV RNA. The binding sites in the 5′-UTR are associated with the facilitation of HCV replication, whereas those in the 3′-UTR are associated with the repression of HCV replication (10). MiR-196 was reported to repress the HCV expression (31).

In the present study, hepatic miR-122 expression was inversely correlated with the severity of functional and histopathological liver damage, serum transaminase levels. MiR-122 has also been reported to be implicated in the regulation of cholesterol and fat metabolism (7, 8, 32, 33). Although the mechanism of miR-122 decrease in injured liver is unknown, it seems that the abundant expression of miR-122 in normal liver becomes decreased as the hepatic injury progresses. MiR-122 is also underexpressed in livers with non-alcoholic steatohepatitis (34). In this study, hepatic miR-122 expression was significantly higher in serum HCV RNA-negative cases than in serum HCV RNA-positive cases. This may also reflect the better hepatic function and less fibrosis in the former than in the latter. In the present study, the hepatic miR-122 expression was inversely correlated with serum transaminase levels and positively correlated with the

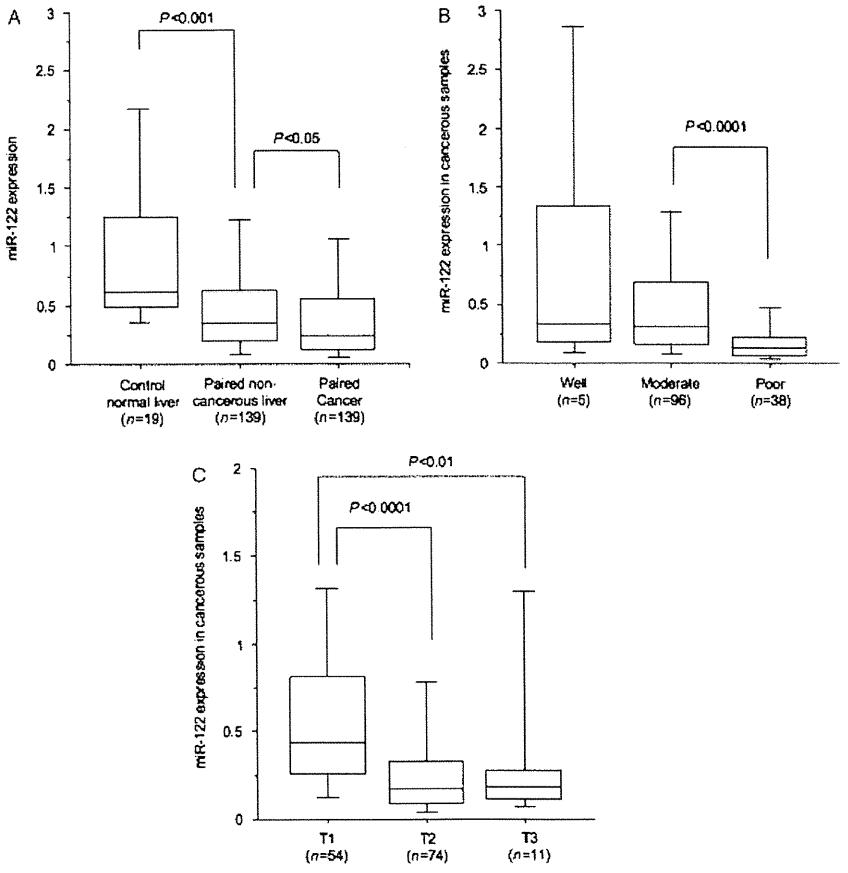

Fig. 7. MicroRNA-122 (miR-122) expression in cancerous and non-cancerous samples. The expression of miR-122 in hepatic cancer was significantly lower than in the paired non-cancerous liver samples ($P < 0.05$) (A). The expression of miR-122 in poorly differentiated hepatic cancer was significantly lower than that in moderately differentiated hepatic cancer ($P < 0.0001$) (B). MiR-122 expression in T2 and T3 cancer samples was significantly lower than that in T1 cancer samples ($P < 0.0001$ and $P < 0.01$ respectively) (C).

serum miR-122 level. Wang *et al.* (35) reported that serum miR-122 levels parallel serum transaminase levels in drug-induced liver injury. The differences between our analyses and Wang's report may be because of whether the liver injury is chronic or acute.

In terms of HCC, decrease of miR-122 in HCC was frequently reported (36–38), which was consistent with our results. Varnholt *et al.* (39) reported that the hepatic expression of miR-122 in HCV-related HCC was higher than that in the normal liver. The differences between our analyses and Varnholt's report may be because of differences in the number or ethnicity of the subjects.

In conclusion, unlike *in vitro*, hepatic miR-122 expression is not correlated with hepatic HCV load in humans. Furthermore, miR-122 expression in cases seronegative for HCV RNA is higher than that in cases seropositive for HCV RNA. Therefore, miR-122 is still potential, but not critical by itself, as a molecular target for HCV therapy. Any therapies for HCV based on miR-122 would need to consider a combination with existing therapies such as IFN therapy, or other potential therapies targeting HCV. MiR-122 is inversely correlated with functional and histopathological liver damage.

Acknowledgements

Financial disclosure: This study was supported in part by a Grant-in-Aid for Scientific Research from the Japan Society of the Promotion of Science, Tokyo, Japan.

Competing interests: None.

References

1. Ambros V. The functions of animal microRNAs. *Nature* 2004; **431**: 350–5.
2. Bartel DP. MicroRNAs: genomics, biogenesis, mechanism, and function. *Cell* 2004; **116**: 281–97.
3. He L, Hannon GJ. MicroRNAs: small RNAs with a big role in gene regulation. *Nature Rev Genet* 2004; **5**: 522–31.

4. Lewis BP, Shih IH, Jones-Rhoades MW, Bartel DP, Burge CB. Prediction of mammalian microRNA targets. *Cell* 2003; **115**: 787–98.
5. Lecellier CH, Dunoyer P, Arar K, *et al.* A cellular microRNA mediates antiviral defense in human cells. *Science* 2005; **308**: 480–1.
6. Lu J, Getz G, Miska EA, *et al.* MicroRNA expression profiles classify human cancers. *Nature* 2005; **435**: 834–8.
7. Lagos-Quintana M, Rauhut R, Yalcin A, *et al.* Identification of tissue-specific microRNAs from mouse. *Curr Biol* 2002; **12**: 735–9.
8. Chang J, Nicolas E, Marks D, *et al.* miR-122, a mammalian liver-specific microRNA, is processed from hcr mRNA and may downregulate the high affinity cationic amino acid transporter CAT-1. *RNA Biol* 2004; **1**: 106–13.
9. Jopling CL, Yi M, Lancaster AM, Lemon SM, Sarnow P. Modulation of hepatitis C virus RNA abundance by a liver-specific microRNA. *Science* 2005; **309**: 1577–81.
10. Jopling CL. Regulation of hepatitis C virus by microRNA-122. *Biochem Soc Trans* 2008; **36**: 1220–3.
11. Randall G, Panis M, Cooper JD, *et al.* Cellular cofactors affecting hepatitis C virus infection and replication. *Proc Natl Acad Sci USA* 2007; **104**: 12884–9.
12. Shan Y, Zheng J, Lambrecht RW, Bonkovsky HL. Reciprocal effects of micro-RNA-122 on expression of heme oxygenase-1 and hepatitis C virus genes in human hepatocytes. *Gastroenterology* 2007; **133**: 1166–74.
13. Chang J, Guo JT, Jiang D, *et al.* Liver-specific microRNA miR-122 enhances the replication of hepatitis C virus in nonhepatic cells. *J Virol* 2008; **82**: 8215–23.
14. Henke JI, Goergen D, Zheng J, *et al.* microRNA-122 stimulates translation of hepatitis C virus RNA. *EMBO J* 2008; **27**: 3300–10.
15. Pedersen IM, Cheng G, Wieland S, *et al.* Interferon modulation of cellular microRNAs as an antiviral mechanism. *Nature* 2007; **18**: 1092–4.
16. Sarasin-Filipowicz M, Krol J, Markiewicz I, Heim MH, Filipowicz W. Decreased levels of microRNA miR-122 in individuals with hepatitis C responding poorly to interferon therapy. *Nat Med* 2009; **15**: 31–3.
17. Takeuchi T, Katsume A, Tanaka T, *et al.* Real-time detection system for quantification of hepatitis C virus genome. *Gastroenterology* 1999; **116**: 636–42.
18. Bedossa P, Poynard T, for the METAVIR Cooperative Study Group. An algorithm for the grading of activity in chronic hepatitis C. *Hepatology* 1996; **24**: 289–93.
19. Edmondson H, Steiner P. Primary carcinoma of the liver: a study of 100 cases among 48,900 necropsies. *Cancer* 1954; **1**: 462–503.
20. International Union Against Cancer (UICC). *TNM Classification of Malignant Tumours*, 6th edn. Hoboken: John Wiley & Sons, 2002.
21. White PA, Pan Y, Freeman AJ, *et al.* Quantification of hepatitis C virus in human liver and serum samples by using LightCycler reverse transcriptase PCR. *J Clin Microbiol* 2002; **40**: 4346–8.
22. Gao L, Aizaki H, He JW, Lai MM. Interactions between viral nonstructural proteins and host protein hVAP-33 mediate the formation of hepatitis C virus RNA replication complex on lipid raft. *J Virol* 2004; **78**: 3480–8.
23. Hamamoto I, Nishimura Y, Okamoto T, *et al.* Human VAP-B is involved in hepatitis C virus replication through interaction with NS5A and NS5B. *J Virol* 2005; **79**: 13473–82.
24. Watashi K, Ishii N, Hijikata M, *et al.* Cyclophilin B is a functional regulator of hepatitis C virus RNA polymerase. *Mol Cell* 2005; **19**: 111–22.
25. Okamoto T, Nishimura Y, Ichimura T, *et al.* Hepatitis C virus RNA replication is regulated by FKBP8 and Hsp90. *EMBO J* 2006; **25**: 5015–25.
26. Wang C, Gale M Jr, Keller BC, *et al.* Identification of FBL2 as a geranylgeranylated cellular protein required for hepatitis C virus RNA replication. *Mol Cell* 2005; **18**: 425–34.
27. Yang W, Hood BL, Chadwick SL, *et al.* Fatty acid synthase is up-regulated during hepatitis C virus infection and regulates hepatitis C virus entry and production. *Hepatology* 2008; **48**: 1396–403.
28. Kapadia SB, Chisari FV. Hepatitis C virus RNA replication is regulated by host geranylgeranylation and fatty acids. *Proc Natl Acad Sci USA* 2005; **102**: 2561–6.
29. Miyanari Y, Atsuzawa K, Usuda N, *et al.* The lipid droplet is an important organelle for hepatitis C virus production. *Nat Cell Biol* 2007; **9**: 1089–97.
30. Lanford RE, Hildebrandt-Eriksen ES, Petri A, Persson R, Lindow M, Munk ME, *et al.* Therapeutic silencing of microRNA-122 in primates with chronic hepatitis C virus infection. *Science* 2010; **327**: 198–201.
31. Hou W, Tian Q, Zheng J, Bonkovsky HL. MicroRNA-196 represses Bach1 protein and hepatitis C virus gene expression in human hepatoma cells expressing hepatitis C viral proteins. *Hepatology* 2010; **51**: 1494–504.
32. Krutzfeldt J, Rajewsky N, Braich R, *et al.* Silencing of microRNAs in vivo with 'antagomirs'. *Nature* 2005; **438**: 685–9.
33. Esau C, Davis S, Murray SF, *et al.* miR-122 regulation of lipid metabolism revealed by in vivo antisense targeting. *Cell Metab* 2006; **3**: 87–98.
34. Cheung O, Puri P, Eicken C, *et al.* Nonalcoholic steatohepatitis is associated with altered hepatic MicroRNA expression. *Hepatology* 2008; **48**: 1810–20.
35. Wang K, Zhang S, Marzolf B, *et al.* Circulating microRNAs, potential biomarkers for drug-induced liver injury. *Proc Natl Acad Sci USA* 2009; **106**: 4402–7.
36. Gramantieri L, Ferracin M, Fornari F, *et al.* Cyclin G1 is a target of miR-122a, a microRNA frequently down-regulated in human hepatocellular carcinoma. *Cancer Res* 2007; **67**: 6092–9.
37. Budhu A, Jia HL, Forgues M, *et al.* Identification of metastasis-related microRNAs in hepatocellular carcinoma. *Hepatology* 2008; **47**: 897–907.
38. Tsai WC, Hsu PW, Lai TC, *et al.* MicroRNA-122, a tumor suppressor microRNA that regulates intrahepatic metastasis of hepatocellular carcinoma. *Hepatology* 2009; **49**: 1571–82.
39. Varnholt H, Drebber U, Schulze F, *et al.* MicroRNA gene expression profile of hepatitis C virus-associated hepatocellular carcinoma. *Hepatology* 2008; **47**: 1223–32.

LIVER TRANSPLANTATION 17:369-372, 2011

ORIGINAL ARTICLE

Coefficient Factor for Graft Weight Estimation from Preoperative Computed Tomography Volumetry in Living Donor Liver Transplantation

Tetsuji Yoneyama,[1] Katsuhiro Asonuma,[2] Hideaki Okajima,[4] Kwang-Jong Lee,[2] Hidekazu Yamamoto,[2] Takayuki Takeichi,[2] Yoshiharu Nakayama,[3] and Yukihiro Inomata[2]

[1]Department of Surgery, Soyo Hospital, Kumamoto, Japan; [2]Department of Pediatric and Transplant Surgery and [3]Department of Diagnostic Radiology, Postgraduate School of Medical Science, Kumamoto University, Kumamoto, Japan; [4]Department of Transplantation and Regenerative Surgery Graduate School of Medical Science, Kyoto Prefectural University of Medicine, Kyoto, Japan

In the clinical setting of living donor liver transplantation (LDLT), it is common to find a discrepancy between the graft volume estimated by preoperative computed tomography volumetry and the actual graft weight (AGW) measured on the back-table. In this study, we attempt to find the coefficient factor that correlates the estimated graft volume to the AGW. Whole livers explanted in 25 LDLT recipients (17 cirrhotic and 8 morphologically normal with familial amyloid polyneuropathy) were evaluated to compare cirrhotic livers and noncirrhotic normal livers. In addition, right lobe grafts (n = 39) and left lobe grafts (n = 35) used in LDLTs were also evaluated to further determine the correlation between estimated graft volume and AGW. The correlation coefficient between estimated liver volume and actual liver weight was 1.01 in whole cirrhotic livers, whereas it was 0.85 in whole livers with familial amyloid polyneuropathy. In the partial liver grafts, it was 0.84 in right lobe grafts and 0.85 in left lobe grafts. In conclusion, we suggest that a correlation coefficient of 0.85 should be applied for the accurate calculation of the graft weight from the volume estimated by preoperative computed tomography in LDLT. ***Liver Transpl 17:369-372, 2011.*** © 2011 AASLD.

Received May 8, 2010; accepted November 26, 2010.

Computed tomography (CT) volumetry plays an important role in predicting graft weights for living donor liver transplantation (LDLT). It is necessary to know the estimated weight of the donor graft before the operation because the ratio of estimated graft weight to recipient's body weight (GRWR) is crucial to planning a successful LDLT.[1-4]

In the past, it has been widely accepted that the density of water was equal to that of liver. In 1985, Van Thiel et al. demonstrated a remarkably close correlation between the liver weight and the volume of water at 25°C, and, hence, liver volume could be converted to liver weight on a one-to-one basis.[5] In other publications, it has been shown that estimated liver volume (ELV) derived from CT volumetry had acceptable accuracy with regards to the actual liver volume (ALV).[6-10] Therefore, CT volumetry has been believed to reliably predict the graft weights and, as such, is widely used for the preoperative evaluation in LDLT. However, a further calculation is thought to be necessary, especially in LDLT donors with healthy livers, because the above concept was derived from the measurement of cirrhotic livers. In actual fact, discrepancies between EGV and actual graft weight (AGW) are often experienced in LDLT even though efforts to decrease the difference between the virtual

Abbreviations: AGW, actual graft weight; ALV, actual liver volume; ALW, actual liver weight; CT volumetry, computed tomography volumetry; ELW, estimated liver weight; EGV, estimated graft volume; ELV, estimated liver volume; FAP, familial amyloid polyneuropathy; GRWR, graft/recipient weight ratio; HTK, histidine-tryptophan-ketoglutarate; LDLT, living donor liver transplantation; UW, University of Wisconsin.

Address reprint requests to Katsuhiro Asonuma, M.D., Department of Pediatric and Transplant Surgery, Postgraduate School of Medical Science, Kumamoto University, 1-1-1 Honjoh Kumamoto, 860-8556 Japan. e-mail: kaso@fc.kuh.kumamoto-u.ac.jp. Telephone: +81-96-373-5618; FAX: +81-96-373-5618; E-mail: kaso@fc.kuh.kumamoto-u.ac.jp

DOI 10.1002/lt.22239
View this article online at wileyonlinelibrary.com.
LIVER TRANSPLANTATION.DOI 10.1002/lt. *Published on behalf of the American Association for the Study of Liver Diseases*

TABLE 1. Characteristics of Recipients With Cirrhotic Livers and FAP Livers

Characteristic	Recipients With Cirrhosis	Recipients With FAP
Number	17	8
Disease (n)	Hepatitis B type (7) Hepatitis C type (7) Primary biliary cirrhosis (1) Primary sclerosing cholangitis (1) Cryptogenic (1)	FAP (8)
Age (average)	51.35	35.13
ELV (mL)	900.82 ± 165.27	1058 ± 260.81
Range (mL)	577.98 ~ 1158.16	751.3 ~ 1523
ALW (g)	885.47 ± 139.83	879.5 ± 178.63
Range (g)	680 ~ 1055	660 ~ 1100

resection line and actual resection line have been made.

Therefore, it is questionable whether 1 mL of liver volume dose actually weighs 1 g. Recently, there have been some studies that dispute the presumed liver density of 1 g/1 mL.[11,12] In this context, we thought it necessary to assess the correlation not only in cirrhotic livers but also in healthy or noncirrhotic livers.

First, we compared the correlation between ELV and ALW using the explanted whole livers from recipients with cirrhosis and recipients without cirrhosis but with familial amyloid polyneuropathy (FAP). In the next step, correlation of EGV and AGW in partial livers that were retrieved from LDLT donors was also evaluated.

PATIENTS AND METHODS

Patients

Twenty five recipients who underwent LDLT in Kumamoto University Hospital, Japan, from December 1998 to January 2006 were randomly selected for the present study. Seventeen recipients with cirrhotic livers and 8 FAP recipients with noncirrhotic livers were enrolled to evaluate whole livers. The characteristics of these recipients are summarized in Table 1. In the same period, 39 right lobe and 35 left lobe grafts used in LDLT were also used for the study (Table 2).

Preoperative Measurement of Liver Volume

Multidetector row CT scanners, General Electric Light Speed Qxi (4DAS multidetector CT) and Philips Brilliance 40 (40DAS multidetector CT), were used to obtain CT images for all recipients and LDLT donors.[13] Images were acquired in 18-20 seconds (arterial phase), 45-60 seconds (portal phase), and 70-80 seconds (hepatic parenchymal phase) after intravenous bolus administration of 120-150 mL nonionic contrast medium (iohexol, omnipaque 300; Daiichi Pharmaceutical, Tokyo, Japan) at a rate of 4-5 mL/second. Images of the hepatic parenchymal phase were used for volume analysis. The volume (in milliliters) was automatically calculated by summation of the products of section thickness and area of the segmented liver in each section with Advantage Workstation version 4.01, as previously reported.[13]

TABLE 2. Characteristics of LDLT Donors for Right Lobe Grafts and Left Lobe Grafts

Characteristic	Right Liver Graft	Left Liver Graft
Number	39	35
EGV (mL)	735.93 ± 134.87	448.41 ± 76.46
Range (mL)	433 ~ 1051	310 ~ 615
AGW (g)	668.75 ± 114.06	415.06 ± 65.43
Range (g)	468 ~ 1032	290 ~ 550

Operative Procedure and Measurement of Actual Liver Weight

In living donor surgery, partial hepatectomy was performed following the cutting plane that was preoperatively imaged. The explanted liver was immediately flushed with histidine-tryptophan-ketoglutarate (HTK) solution or University of Wisconsin (UW) solution at 4°C. After the solution was drained completely from the liver, the AGW or actual liver weight (ALW) was measured in grams by an automatic weighing machine. Whole livers explanted from FAP recipients were flushed in the same manner as other partial grafts with UW solution to be used as grafts for domino recipients.

Statistical Analysis

Values are shown as mean ± standard deviation. Statistical analysis was performed using SPSS version 11.0 (SPSS Inc., Chicago, IL). A value of $P < 0.05$ was considered significant. The regression line between ELV and ALW was determined by use of regression analysis, and confidence interval for every correlation coefficient was 95%.

RESULTS

Correlation Between ELV and ALW of Whole Liver

In cirrhotic whole liver, ELV averaged 900.82 ± 165.27 mL and ranged from 577.98-1158.16 mL. The mean ALW was 885.47 ± 139.83 g and ranged from 680-1055 g. The relationship between ELV and ALW was significantly linear ($Y = 1.01X$, $r^2 = 0.88$; $P < 0.001$; Fig. 1). In noncirrhotic FAP liver, the ELV averaged 1058 ± 260.81 mL and ranged from 751.3-1523 mL. The ALW averaged 879.5 ± 178.63 g and ranged from 660-1100 g and in this case too, the relationship between ELV and ALW was linear ($Y = 0.85X$, $r^2 = 0.99$; $P < 0.001$; Fig. 2). Liver density of cirrhotic liver was found to be consistent with 1 g/1 mL and in accordance with previous reports. However, in the noncirrhotic FAP livers, the density was 0.85 g/1 mL.

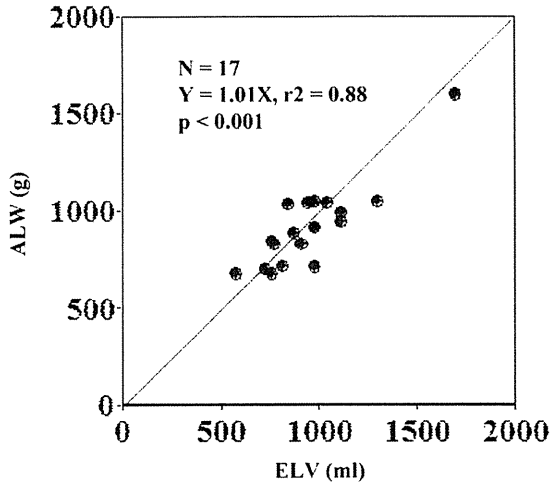

Figure 1. Correlation between ELV and ALW of whole liver in patients with cirrhosis. There was an excellent correlation (r^2 = 0.88, slope: 1.01, $P < 0.001$).

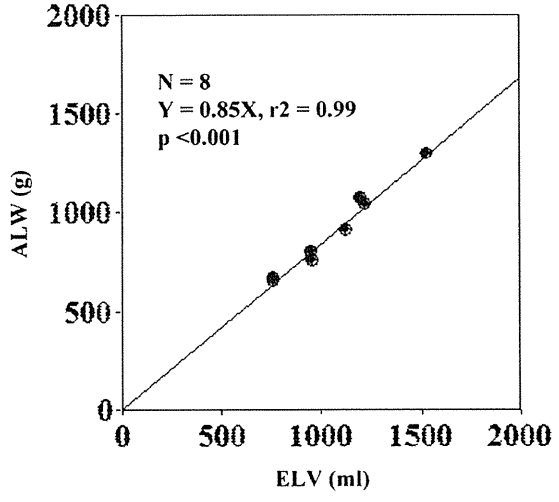

Figure 2. Correlation between ELV and ALW of whole liver in FAP patients. There was an excellent correlation (r^2 = 0.99, slope: 0.85, $P < 0.001$).

Correlation Between EGV and AGW of Graft Livers in LDLT Donors

The EGV of right lobe grafts averaged 735.93 ± 134.87 mL with a range of 433-1051 mL. The AGW averaged 668.75 ± 114.06 g and ranged from 465 to 1035 g. The correlation between EGV and AGW was linear (Y = 0.84X, r^2 = 0.52; $P < 0.01$; Fig. 3A). The EGV of the left lobe averaged 448.41 ± 76.46 mL and ranged from 310-615 mL. The AGW averaged 415.06 ± 65.43 g and ranged from 290-550 g. The correlation between EGV and AGW was significantly linear (Y = 0.85X, r^2 = 0.82; $P < 0.01$; Fig. 3B). Hence, the coefficient of weight per volume was 0.84 in right lobe grafts ($P < 0.01$) and 0.85 in left lobe grafts ($P < 0.01$).

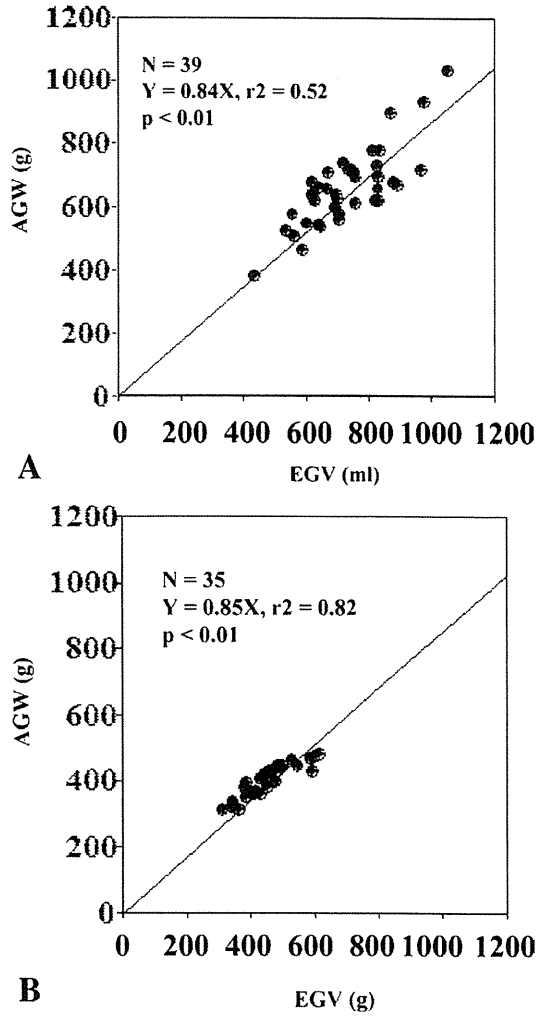

Figure 3. Correlation between EGV and AGW in healthy donors. (A) Right lobe grafts (r^2 = 0.52, slope: 0.84, $P < 0.01$), (B) Left lobe grafts (r^2 = 0.82, slope: 0.85, $P < 0.01$).

DISCUSSION

In Japan, where liver grafts from deceased donors have been lacking, LDLT has been the dominant option. Graft size is an important component of both the donor evaluation and the outcome of LDLT. The experience with LDLT by Kiuchi et al. suggested that a patient with a GRWR of less than 0.8% had a significantly lower chance of survival.[3] On the other hand, Ben-Haim et al.[4] reported that recipients with Child-Pugh grade A or recipients without cirrhosis could probably tolerate a GRWR up to 0.6%. Recently, it has been shown that grafts with GRWR of less than 0.8% could produce the same results as grafts with GRWR of more than 0.8% with innovative surgical techniques.[15,16] Whichever technique is used, the graft weight measured at harvesting is used for the calculation of the GRWR. Therefore, accurate estimation of the graft weight from the EGV by preoperative CT imaging is important because the estimated

GRWR is necessary to decide if the LDLT is feasible and what type of graft should be used, for instance, a right lobe graft or a left lobe graft. The calculation for conversion from volume to the weight has been conventionally based on the classical concept that 1 mL of liver volume is equal to 1 g of liver weight that Van Thiel et al. demonstrated.[5] However, the measurements in that study were performed with cirrhotic livers.[6-10] Evaluation of the weight of noncirrhotic livers by volume measured by CT has not previously been performed. Some reports have revealed that the error ratio of the estimation of the weight by preoperative CT volumetry ranged from ± 5% to ± 20%.[11] Several possible reasons causing the discrepancy have been considered, such as blood flow, anatomy, CT machine variation, interobserver variations, and so on. However, only a few have stressed the necessity to correct the estimation of liver weight derived from CT volumetric measurement.[11,12] We selected the explanted FAP liver as a specimen of the noncirrhotic liver because the FAP liver is morphologically the same as normal liver even though it produces atypical transthyretin.[14]

In this study, it has been elucidated that the specific gravity of cirrhotic liver was significantly different from that of noncirrhotic liver. The result derived from the cirrhotic livers in our study was consistent with the view that 1 mL of the liver volume equals 1 g of liver weight, as demonstrated by Van Thiel et al. (Fig. 1). However, in noncirrhotic livers (ie, FAP livers), 0.85 g of liver weight was equal to 1 mL of liver volume (Fig. 2). These results suggest that it might be necessary to multiply the value of EGV by 0.85 to calculate the estimated weight of the liver graft in LDLT. Interestingly, the correlation coefficients between EGV and AGW in right lobe grafts and left lobe grafts were 0.84 and 0.85, respectively (Fig. 3). These figures were very similar to that of FAP livers and further support our findings.

The coefficient factor (0.85), as an absolute value, might not always be applicable in other institutions because of several biases, such as the differences in CT machines, calculation software, preservation solution, ethnicity, sex, and so on. In fact, each institution might have its own coefficient factor. However, the fact that the density of normal liver is lower than that of cirrhotic liver should be realized.

In this study, HTK solution or UW solution was used as perfusion fluid in grafts. HTK solution may cause more edema in the liver than UW solution; however, because the grafts were weighed immediately after being flushed out, we feel that the influence of the difference between the solutions was minimized. There was a small difference between right lobe grafts and left lobe grafts in terms of the value of r^2. This may have been due to a difference in the accuracy of the cutting line, depending on whether the middle hepatic vein was included in the graft.

In conclusion, in our institution, the weight of the liver graft in LDLT can be estimated preoperatively by multiplying the EGV by 0.85.

REFERENCES

1. Inomata Y, Kiuchi T, Kim I, Uemoto S, Egawa H, Asonuma K, et al. Auxiliary partial orthotopic living donor liver transplantation as an aid for small-for-size graft in larger recipients. Transplantation 1999;67:1314–1319.
2. Sakamoto S, Uemoto S, Uryuhara K, Kim I, Kiuchi T, Egawa H, et al. Graft size assessment and analysis of donors for living donor liver transplantation using right lobe. Transplantation 2001;71:1407–1413.
3. Kiuchi T, Kasahara M, Uryuhara K, Inomata Y, Uemoto Y, Asonuma K, et al. Impact of graft size mismatching on graft prognosis in liver transplantation from living donors. Transplantation 1999;67:321–327.
4. Ben-Haim M, Emre S, Fishbein TM, Sheiner PA, Bodian CA, Kim-Schluger L, et al. Critical graft size in adult-to-adult living donor liver transplantation: impact of the recipient's disease. Liver Transpl 2001;7:948–953.
5. Van Thiel DH, Hagler NG, Schade RR, Skolnick ML, Pollitt Heyl A, Rosenblum E, et al. In vivo hepatic volume determination using sonography and computed tomography. Gastroenterology 1985;88:1812–1817.
6. Urata K, Kawasaki S, Matsunami H, Hashikura Y, Ikegami T, Ishizone S, et al. Calculation of child and adult standard liver volume for liver transplantation. HEPATOLOGY 1995;21:1317–1321.
7. Schiano TD, Bodian C, Schwartz ME, Glajchen N, Min AD. Accuracy and significance of computed tomographic scan assessment of hepatic volume in patients undergoing liver transplantation. Transplantation 2000;69:545–550.
8. Kamel IR, Kruskal JB, Warmbrand G, Goldberg SN, Pomfret EA, Raptopoulos V, et al. Accuracy of volumetric measurements after virtual right hpatectomy in potential donors undergoing living adult liver transplantation. AJR Am J Roentgenol 2001;176:483–487.
9. Harada N, Shimada M, Yoshizumi T, Suehiro T, Soejima Y, Maehara Y. A simple and accurate formula to estimate left hepatic graft volume in living-donor adult liver transplantation. Transplantation 2004;77:1571–1575.
10. Salvalaggio PR, Baker TB, Koffron AJ, Fryer JP, Clark L, Superina RA, et al. Liver graft volume estimation in 100 living donors: measure twice, cut once. Transplantation 2005;80:1181–1185.
11. Lemke AJ, Brinkmann MJ, Schott T, Niehues SM, Settmacher U, Neuhaus P, Felix R. Living donor right liver lobes: preoperative CT volumetric measurement for calculation of intraoperative weight and volume. Radiology 2006;240:736–742.
12. Hwang S, Lee SG, Kim KH, Park KM, Ahn CS, Moon DB, et al. Correlation of blood-free graft weight and volumetric graft volume by an analysis of blood content in living donor liver grafts. Transplant Proc 2002;34:3293–3294.
13. Nakayama Y, Li Q, Katsuragawa S, Ikeda R, Hiai Y, Awai K, et al. Automated hepatic volumetry for living related liver transplantation at multisection CT. Radiology 2006; 240:743–748.
14. Takei Y, Ikeda S, Ikegami T, Hashikura Y, Miyagawa S, Ando Y, et al. Ten years of experience with liver transplantation for familial amyloid polyneuropathy in Japan: outcome of living liver transplantations. Intern Med 2005;144:1151–1156.
15. Selzner M, Kashfi A, Cattral MS, Selzner N, Greig PD, Lilly L, et al. A graft to body weight ratio less than 0.8 does not exclude adult-to-adult right-lobe living donor liver transplantation. Liver Transpl 2009;15:1776–1782.
16. Ikegami T, Matsuda Y, Ohno Y, Mita A, Kobayashi A, Urata K, et al. Prognosis of adult patients transplanted with liver grafts <35% of their standard liver volume. Liver Transpl 2009;15:1622–1630.

Transplantation of Liver Organoids in the Omentum and Kidney

*Ryota Saito, *Yuji Ishii, *Ryusuke Ito, †Keisuke Nagatsuma, †Ken Tanaka, ‡Masaya Saito, §Haruka Maehashi, §Hideki Nomoto, §Kiyoshi Ohkawa, **Hiroshi Mano, ††Mamoru Aizawa, †Hiroshi Hano, *Katsuhiko Yanaga, and ‡‡Tomokazu Matsuura

*Departments of *Surgery, †Pathology, ‡Internal Medicine, §Biochemistry, Jikei University School of Medicine, Tokyo; **Clinical Dietetics, Faculty of Pharmaceutical Sciences, Josai University, Saitama; ††Department of Industrial Chemistry, School Science and Technology, Meiji University; and ‡‡Department of Laboratory Medicine, Jikei University School of Medicine, Tokyo, Japan*

Abstract: Liver organoids were reconstructed by mouse-immortalized hepatocytes and nonparenchymal cells (sinusoidal endothelial cells and hepatic stellate cells) in a radial-flow bioreactor (RFB). A biodegradable apatite-fiber scaffold (AFS) was used as a scaffold packed in the RFB, which enables three-dimensional cell cultures. The organoids cocultured in the RFB showed a liver-like structure with high-density layers of hepatocytes and the formation of vessel-like structures. A liver organoid consisting of three cocultured cells was transplanted under the kidney capsule (kidney group) or into the omentum (omentum group) using BALB/c nude mice. Transplanted liver organoids survived in the kidney or omentum. The expression of mRNAs of albumin, connexin 26 and 32, hepatocyte nuclear factor 4α, and glucose-6-phosphatase was increased in both groups at 8 weeks after transplantation in comparison to the pretransplant status. Tyrosine aminotransferase appeared only in the omentum group. The results suggested that the functions of liver organoids differed depending on the transplanted site in the recipient animals. **Key Words:** Liver organoid—Radial-flow bioreactor—Co-culture—Transplantation—Immortalized hepatocyte.

doi:10.1111/j.1525-1594.2010.01049.x

Received September 2009; revised February 2010.

Address correspondence and reprint requests to Dr. Tomokazu Matsuura, Department of Laboratory Medicine, The Jikei University School of Medicine, 3-25-8 Nishi-shinbashi, Minato-ku, Tokyo 105-8461, Japan. E-mail: matsuurat@jikei.ac.jp

Liver transplantation is an established treatment for end-stage hepatic failure. However, the bioartificial liver (BAL) is attracting attention as an alternative. A previous study demonstrated the efficacy of a radial-flow bioreactor (RFB) system combined with extracorporeal circulation in a porcine model of acute hepatic failure (1). Extracorporeal BAL may thus potentially be useful as a temporary support for patients presenting with acute hepatic failure. However, new methods are needed for long-term hepatic support in patients with chronic liver failure. Accordingly, a treatment for chronic liver failure was established using implantable artificial liver tissue (liver organoid) produced by tissue engineering (2,3). This treatment was designed to provide long-term support by transplanting liver organoids into patients. As a preliminary study, we first tried to produce liver organoids using a coculture of immortalized mouse hepatocytes (IMHs), hepatic stellate cells (HSCs), and sinusoidal endothelial cells (SECs) in apatite fiber scaffold (AFS) (4). The study next investigated whether the liver organoids could be transplanted into the omentum and under the kidney capsule in nude mice.

MATERIALS AND METHODS

Construction of liver organoids

IMH-4 cells, immortalized mouse HSCs (A7), and SECs (M1) were established from H-2Kb-tsA58 mice (Charles River Laboratories, Inc., Wilmington, MA, USA), which were transfected with the temperature-sensitive large T-antigen of the SV40 gene (5–7). The RFB system included a 5-mL RFB (RA-5; ABLE, Tokyo, Japan), mass flow controller, and a reservoir (2,3) (Fig. 1A). The AFS scaffold was formed from hydroxyapatite fibers with long axis dimensions of 100–200 μm (4). AFSs have consecutive pores with a diameter of 250 μm (Fig. 1B). Each single-crystal apatite fiber possesses two crystalline facets (facets A and C), and the fibers are biodegradable because much of facet A is exposed (4). AFS was packed into

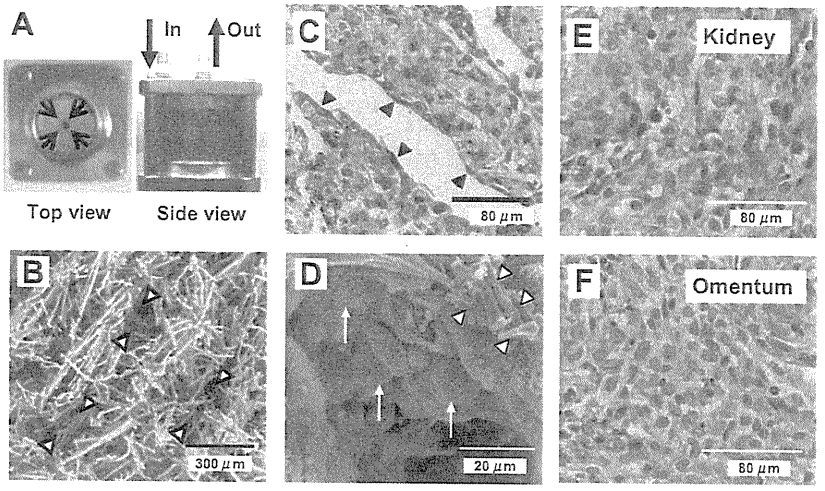

FIG. 1. (A) The RFB chamber. The culture fluid perfused the cylindrical chamber in the direction shown by the large arrows. Culture fluid flows radially from the periphery to the center, as shown by the small arrows. AFS is packed inside the chamber. (B) SEM observation of the AFS. A maze of channels (arrowheads) with a diameter of 250 μm is observed inside the carrier. (C) H&E-stained image of a sample from the RFB coculture group. The surface is covered with flat cells (arrowheads). (D) SEM images of a sample from the RFB coculture group. The arrowheads show single apatite fibers. Hepatocytes (arrows) with microvilli are infiltrating into the channels and proliferating three-dimensionally. (E, F) Histological findings of transplanted tissue. H–E staining of an RFB coculture group organoid transplanted under the renal capsule (E) and to the omentum (F). Proliferation of cuboidal immortalized hepatocytes is observed at both sites.

the RFB and the culture medium perfused the chamber radially from the periphery to the center (Fig. 1A). ASF 104 medium (Ajinomoto Co. Ltd., Tokyo, Japan) with 2% FBS was used as the culture fluid (2). The following three groups were compared. (i) RFB coculture group: coculture of IMH-4, M1, and A7 cells in the RFB system; (ii) RFB IMH-4 group: culture of IMH-4 cells alone in the RFB system; and (iii) IMH-4 dish group: a monolayer culture of IMH-4 in a dish. In the RFB coculture group, 1×10^7 IMH-4 cells were added to the reservoir and perfused for 2 h as a closed circuit to allow the cells to attach to the scaffold. A7 cells (1×10^7) were added on day 8 and M1 cells (3.3×10^6) were added on day 13. The RFB was opened on day 17.

Transplantation of liver organoids

The animal experiment was performed with the approval of the Jikei University Animal Care Committee. Six-week-old BALB/cAJcl nude mice (CLEA Japan, Inc., Tokyo, Japan) were used as recipients. Two types of organoid from the RFB coculture group and RFB IMH-4 group were transplanted. Pentobarbital sodium (1–1.5 mg/body) was administered intraperitoneally before transplantation. The kidney group ($n = 5$) underwent transplantation of an organoid measuring 2.5 mm into a pocket under the renal capsule, and the omentum group ($n = 5$) underwent transplantation of an organoid measuring 2.8 mm into the porta-hepatis region and covered with gastro-colic omentum. The animals were sacrificed at 4 or 8 weeks after transplantation.

Histological examination

A histological examination was performed for the RFB coculture group and the organoids at 8 weeks after transplantation. Specimens were fixed with 10% buffered formalin and embedded in paraffin. Then sections of 5 μm in thickness were prepared and stained with hematoxylin and eosin (H&E).

Scanning electron microscopy (SEM)

The organoids of the RFB coculture group were observed by SEM, and the methods have been described previously (2,7).

Reverse transcriptase polymerase chain reaction (RT-PCR)

The expression of mRNA was analyzed by RT-PCR in the IMH-4 dish group, RFB IMH-4 group, RFB coculture group, and the organoids harvested at 4 or 8 weeks. The cells were lysed and mRNA was extracted with the RNeasy mini kit (Qiagen, Hilden, Germany). cDNA was synthesized from 1 μg of total RNA using an oligo-p (dT) 15 primer and 1 ST standard cDNA synthesis Kit (Roche Diagnostics Corp., Switzerland) according to the manufacturer's instructions. Then cDNA for

liver-related factors was amplified by the PCR method: The primers were as follows: albumin/(sense)5′-ttcgctacacccagaaagca-3′,(antisense)5′-ggtttggacccctcagtcgag-3′; connexin26(Cx26)/(sense)5′-aaggaggtgtggggagatga-3′,(antisense)5′-gcctggaaatgaagcagtcc-3′; connexin32(Cx32)/(sense)5′-tcagggacactgtggtggac-3′,(antisense)5′-cggcgcagtatgtctttcag-3′; hepatocyte nuclear factor 4α(HNF-4α)/(sense)5′-acgtgctgctcctaggcaat-3,(antisense)5′-gtgcccatgtgttcttgcat-3′; tyrosine aminotransferase(TAT)/(sense)5′-ccctgtggctctgtgttcag-3′,(antisense)5′-ggagtccaggaatggcagac-3′; glucose-6-phosphatase(G6Pase)/(sense)5′-tccggtgtttgaacgtcatc-3′,(antisense)5′-tccggtacatgctggagttg-3′; β-actin/(sense)5′-accacagctgagagggaaatcg-3′,(antisense)5′-agaggtctttacggatgtcaacg-3′. β-actin was used as control.

RESULTS AND DISCUSSION

Morphology of liver organoids and transplanted liver organoids

Cellular transplantation has been attempted at various extrahepatic sites, but the transplantation of hepatocytes alone resulted in a loss of cellular functions (8,9). Therefore, the tissue engineering technique was investigated and various scaffolds have been tested (10). AFS was used as a scaffold in the current study, and IMH-4, M1, and A7 cells were employed to prepare liver organoids by culture in an RFB system. H&E staining of cultures showed that rounded IMH-4 cells formed high-density layers, while the surface was covered with flat cells and vessel-like structures were present (Fig. 1C). SEM showed cellular infiltration into the channels of the apatite fiber grid and three-dimensional proliferation. The cultured immortalized hepatocytes were hemispheric and microvilli were observed (Fig. 1D). H&E staining revealed proliferation of hepatocytes when the RFB coculture group was transplanted (Fig. 1E,F). In contrast, fibrosis and necrosis were seen when the RFB IMH-4 group was transplanted. The construction of the vascular network is indispensable for the stabilization of transplanted organoids (11). Coculture with M1 and A7 cells may contribute to construction of the vascular network and engraftment of a liver organoid.

Gene expression in liver organoids and transplanted liver organoids

An enhanced gene expression of Cx 26 & 32 and TAT was observed in the RFB coculture group in comparison with the dish culture of hepatocytes (Fig. 2A). Improvement of various liver functions is generally expected to occur with coculture in comparison with monoculture (12,13), but the gene expression of albumin was lower in the coculture RFB organoids in comparison with the dish culture. HNF-4α, which regulates albumin synthesis, was also decreased. This result is similar to the repression of albumin release from human hepatocellular carcinoma cocultured with M1 and A7 in RFB (2). Therefore, the albumin production is regulated at the gene expression and transcriptional level in a complicated manner, and it is very difficult to elucidate which factor will affect albumin gene expression (14,15). One reason for the down regulation may be that immortalized cells are not appropriate for the RFB system. Immortalized cells may change the characteristics of its original cells depending on the culture conditions.

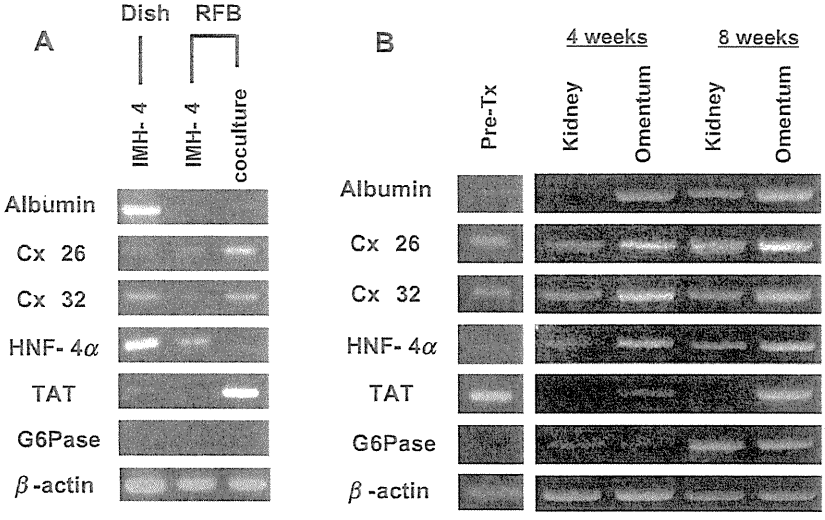

FIG. 2. (A) Pretransplantation. Expression of mRNA for liver-specific genes was compared among the IMH-4 dish group, RFB IMH-4 group, and RFB coculture group. Cx 26 and 32 and TAT were more strongly expressed in the RFB coculture group, but the expression of albumin and HNF-4α was decreased in comparison with the IMH-4 dish group. (B) Posttransplantation. The expression of mRNA for liver-specific genes was compared at 4 or 8 weeks after transplantation of RFB coculture group. Cx 26 and 32 were expressed after transplantation to both sites. Albumin, HNF-4α, and G6Pase expression were stronger at 8 weeks after transplantation in comparison with that before transplantation. TAT was only expressed in the liver organoids transplanted to the omentum. TX., transplantation.

Extrahepatic sites for liver organoid transplantation were investigated in this study because the goal was to transplant a certain number of cells (organoid) in a single operation. The renal capsule is a useful site because of weak graft rejection and development of a vascular network (11,16). The omentum is also a useful site for transplantation (17). Gene expression of albumin, HNF-4α, and G6Pase was stronger at 8 weeks in comparison with that before transplantation in both sites (Fig. 2B). Interestingly, the expression of the TAT gene at 8 weeks was only re-expressed when organoids were implanted in the omentum. This site is likely to be influenced by hepatotrophic substances such as insulin and glucagon due to its anatomical position and structure (8,17), and such influences may be related to the difference of TAT expression.

CONCLUSIONS

Liver-like organoids of immortalized cells can therefore be constructed using RFB culture with a biocompatible AFS. Cocultured grafts with vessel-like structures only survived in the kidney and omentum of nude mice. The functions of liver organoids differed depending on the transplanted site in the recipient animals. These results confirm the efficacy of using liver organoids as a transplantable cell source.

Acknowledgments: The authors thank Mr. Hideaki Saito and Mrs. Emi Kikuchi of the DNA Medical Institute at the Jikei University. This study was supported in part by grants from University Start-Ups Creation Support System, Ministry of Education, Culture, Sports, Science and Technology (#18390371) and by the Program for Promotion of Fundamental Studies in Health Sciences of the National Institute of Biomedical Innovation.

REFERENCES

1. Kanai H, Marushima H, Matsuura T, et al. Extracorporeal bioartificial liver using the radial-flow bioreactor in treatment of fatal experimental hepatic encephalopathy. *Artif Organs* 2007;31:148–51.
2. Saito M, Matsuura T, Masaki T, et al. Reconstruction of liver organoid using a bioreactor. *World J Gastroenterol* 2006;12: 1881–8.
3. Saito M, Matsuura T, Nagatsuma K, et al. The functional interrelationship between gap junctions and fenestrae in endothelial cells of the liver organoid. *J Membr Biol* 2007;217:115–21.
4. Hiramoto H, Aizawa M. Three-dimensional cell culture of hepatocytes using apatite-fiber scaffold and application to a radial-flow bioreactor. *Archiv BioCeramics Res* 2006;6:220–3.
5. Yanai N, Suzuki M, Obinata M. Hepatocyte cell lines established from transgenic mice harboring temperature-sensitive simian virus 40 large T-antigen gene. *Exp Cell Res* 1991;197: 50–6.
6. Matsuura T, Kawada M, Shimizu H. *Vitamin A Metabolism of Immortalized Hepatic Stellate Cells in the Bioreactor. Cells of the Hepatic Sinusoid 7.* Leiden: Kupffer Cell Foundation, 1999;88–9.
7. Matsuura T, Kawada M, Hasumura S, et al. High density culture of immortalized liver endothelial cells in the radial-flow bioreactor in the development of an artificial liver. *Int J Artif Organs* 1998;21:229–34.
8. Ricordi C, Lacy PE, Callery MP, et al. Trophic factors from pancreatic islets in combined hepatocyte-islet allografts enhance hepatocellular survival. *Surgery* 1988;105:218–23.
9. Ohashi K, Park F, Kay MA. Hepatocyte transplantation: clinical and experimental application. *J Mol Med* 2001;79:617–30.
10. Davis MW, Vacanti JP. Toward development of an implantable tissue engineered liver. *Biomaterials* 1996;17:365–72.
11. Ohashi K, Waugh JM, Dake MD, et al. Liver tissue engineering at extrahepatic sites in mice as a potential new therapy for genetic liver diseases. *Hepatology* 2005;41:132–40.
12. Goulet F, Normand C, Morin O. Cellular interactions promote tissue-specific function, biomatrix deposition and junctional communication of primary cultured hepatocytes. *Hepatology* 1988;8:1010–8.
13. Guguen-Guillouzo C, Clement B, Baffet G, et al. Maintenance and reversibility of active albumin secretion by adult rat hepatocytes co-cultured with another liver epithelial cell type. *Exp Cell Res* 1983;143:47–54.
14. Arias IM, Boyer JL, Jakoby WB, et al. *The Liver. Biology and Pathobiology*, 3rd Edition. New York: Raven Press, Ltd., 1994.
15. Masaki T, Matsuura T, Ohkawa K, et al. All-trans retinoic acid down-regulates human albumin gene expression through the induction of C/EBPbeta-LIP. *Biochem J* 2006;397:345–53.
16. Bakeine GJ, Bertolotti A, Latina M, et al. Surface properties and implantation site affect the capsular fibrotic overgrowth. *J Biomed Mater Res A* 2007;83:965–9.
17. Lee H, Cusick RA, Utsunomiya H, et al. Effect of implantation site on hepatocytes heterotopically transplanted on biodegradable polymer scaffolds. *Tissue Eng* 2003;9:1227–32.

肝臓　52巻1号　36-41（2011）

＜症例報告＞

生体肝移植の待機中に脾梗塞を認めた原発性胆汁性肝硬変の1例

原　裕子　北　嘉昭*　脇山　茂樹　後町　武志　坂本　太郎
広原　鍾一　石田　祐一　三澤　健之　矢永　勝彦

要旨：脾梗塞は比較的稀な疾患であるが，門脈圧亢進症による巨脾を有する末期肝硬変患者に稀に発症することが知られている．症例は44歳女性，原発性胆汁性肝硬変のため生体肝移植を目的に当科入院中，突然の左側腹部痛，39℃の発熱を訴え，造影CTで脾臓に楔状の造影不良領域を認めたため脾梗塞と診断した．保存的治療により病状が改善し，1週間後，予定通り生体肝移植，脾摘術を施行した．術後経過は良好で，患者は15病日に退院した．摘出された脾臓の重量は1,120 gであり，肉眼的に脾梗塞を認め，病理組織学的検索でも細小動静脈に梗塞巣が多発し，好中球浸潤が認められた．一方，線維化，ヘモジデリン沈着が認められなかったため，1週間前に起こった新しい梗塞巣と診断した．以上より，門脈圧亢進症による巨脾を有する患者が左側腹部痛や炎症症状を訴えた場合，脾梗塞を疑い，適切な治療を選択すべきであると考えられた．

索引用語：　脾梗塞　　原発性胆汁性肝硬変　　巨脾　　生体肝移植

はじめに

原発性胆汁性肝硬変（以下PBC）では蛋白合成能などの肝機能が比較的保たれている病初期から門脈圧亢進症とそれに付随した脾機能亢進症が存在することが稀ではない．Zeegenら[1]は，PBC 23例中17例（74%）で組織学的に肝硬変を認めなかったにもかかわらず，15例（65%）に食道静脈瘤からの出血を初発症状として認めたと報告し，その機序として肝内の細胆管周囲の炎症によるintrahepatic presinusoidal blockの可能性を示唆している．わが国においてもPBCの自然史や合併症については多くの報告があり，病初期においては進行が緩やかであるが，食道静脈瘤などの門脈圧亢進症を主たる兆候として発症する場合（portal hypertensive-type progression）があることが知られている[2][3]．

一方，脾梗塞は血液疾患や血栓症に関連して起こる例が多い[4]が，門脈圧亢進症や巨脾を有する症例に頻度が高いことも知られている[5]．Jarochら[4]の報告では，門脈圧亢進症がその成因と考えられたのは，脾梗塞患者152例中3例（2%）のみであったとしている．さらに，筆者らが国内外の文献を検索しえた限りでは門脈圧亢進症を有すると考えられる末期肝硬変患者に脾梗塞が起こった症例報告は6例のみであった[6]~[9]．今回，筆者らは，生体肝移植の待機中に脾梗塞を合併したPBCの1例を経験したので，文献的考察を加え報告する．

東京慈恵会医科大学外科学講座消化器外科
*Corresponding author: kita@jikei.ac.jp

＜受付日2010年8月5日＞＜採択日2010年11月19日＞

症　例

患者：44歳，女性．

主訴：発熱，左側腹部痛．

既往歴：31歳　CREST症候群，34歳　Sjögren症候群，36歳　食道静脈瘤治療（EVL），骨折歴（－）．

家族歴：父　胃癌，叔母　関節リウマチ，叔父　マクログロブリン血症．

嗜好歴：喫煙歴・飲酒歴なし．

現病歴：1995年より肝機能障害を指摘され，PBCと診断された．2008年5月より腹水貯留及び全身倦怠感を認め，実兄をドナーとする生体肝移植を希望され，2008年11月に当科入院となった．PBCに対する肝移植の適応としては，Tableに示すように，T-Bil：3.7 mg/dL，AST：142 IU/L，ALT：77 IU/L，Cr：0.79 mg/dL，PT：65%（INR：1.3），MELD score（http://www.mayoclinic.org/meld/mayomodel6.html）は14点であったが，日本肝移植適応研究会のPBCの予後予測式[10]にて6カ月後の予想死亡率が51%と基準の50%を超

Table

WBC	4,200 /μL	TP	7.4 g/dL
Lympho	15.6 %	Alb	3.1 g/dL
Mono	4.9 %	T-Bil	3.7 mg/dL
Neutro	79.3 %	D-Bil	2.0 mg/dL
Baso	0.2 %	AST	142 IU/L
Eosino	0 %	ALT	77 IU/L
RBC	309×10^4 /μL	LDH	245 IU/L
Hb	9.1 g/dL	ChE	1,274 mU/mL
Ht	28.2 %	ALP	387 IU/L
Plt	3×10^4 /μL	γ-GTP	225 IU/L
		BUN	18 mg/dL
PT	65 %	Cr	0.79 mg/dL
	16.1 sec	Na	136 mmol/L
PT-INR	1.3	K	4.4 mmol/L
APTT	47.6 sec	Cl	99 mmol/L
Fbg	352 mg/dL	CRP	3.01 mg/dL

えているため適応ありと判断した．また，本症例では門脈圧亢進症が強く，食道静脈瘤破裂の危険や脾機能亢進症，QOL の低下なども考えると，移植の時期として早くはないと判断した．2008 年 12 月に移植予定であったが，誤嚥性肺炎を発症し，2009 年 1 月に延期となり移植手術待機中であった．

入院時身体所見：身長 161 cm，体重 44 kg，血圧 98/54 mmHg，脈拍 120・整，眼瞼結膜に貧血，眼球結膜に黄染を認めた．腹部平坦・軟．肝脾腫を認めた．表在リンパ節は触知せず．

治療経過：上記のごとく肺炎は治癒したが，生体肝移植予定日の 7 日前に突然 39℃ の発熱及び左側腹部痛を認めた．症状発現当日の血液検査所見を Table に示す．炎症のマーカーも上昇したため，抗生物質（PIPC）の点滴静注で治療を開始した．同日に静脈血，尿の培養に加えてインフルエンザ抗原の検索を行ったが，血液培養は陰性，尿培養は Gram Positive Rod 1＋，インフルエンザ抗原は A－B－で，いずれも感染の原因とは考えられなかった．症状発現時から生体肝移植までの経過を Fig. 1 に示す．胸部 CT では，2008 年 12 月の誤嚥性肺炎時に認めた肺の浸潤影所見は認めなかった．さらに，腹部の感染巣の検索目的で施行した腹部造影 CT（Fig. 2）では，脾臓下極に楔状の造影不良領域を認め，脾梗塞と診断した．その際，以前から指摘されていた最大径 15 mm の脾動脈瘤には変化を認めなかった（Fig. 3）．

脾梗塞の臨床症状が改善したので，予定通り 2009 年 1 月に血液型の一致する兄をドナーとする生体肝移植手術を行った．ドナーの中肝静脈を含めた左葉グラフト（重量は 433 g，レシピエントの標準肝容積の 42.7%）を同所性に移植した．手術時間は 723 分で出血量は 1,850 g であった．摘出した病的肝，脾臓の重量は各 1,100 g，1,120 g であった．術後経過はドナー，レシピエントともに良好で，それぞれ術後 10，15 日で退院した．

脾臓は巨脾で肉眼的に下極を中心に梗塞所見を呈しており，組織学的にも細小動静脈に梗塞巣が多発し，好中球浸潤が認められた．また，線維化やヘモジデリン沈着は認められなかった．さらに，脾臓には上記以外の陳旧性の梗塞巣が認められなかった．以上より，脾梗塞巣は 1 週間前に発症した新規の単発の病変であると診断した．

考　察

脾梗塞は主として脾動脈の脾内分枝の塞栓により脾臓の 1 区域が壊死に陥ったものである．脾梗塞の原因について，Jaroch[4] らは 10 年間で経験した 75 例の自験例に文献上報告された 77 例を加えた 152 例で review を行っている．彼らの報告では 40 歳前の脾梗塞の症例では，何らかの血液疾患に関連して起こり（全体の 29%），40 歳以後の症例では，心疾患などに関連した血栓症に起因する例が全体の 38% と，主たる原因と報告している．

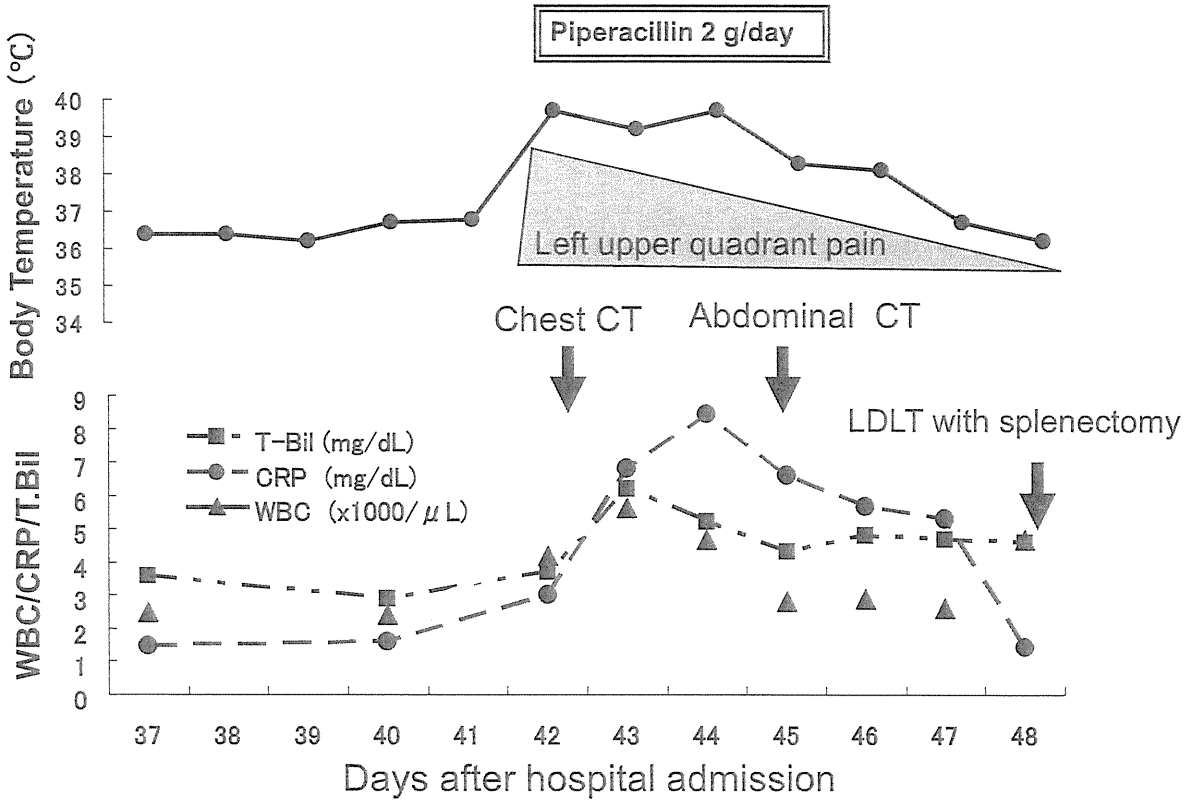

Fig. 1 Clinical course of the patient before and after splenic infarction. LDLT＝Living Donor Liver Transplantation

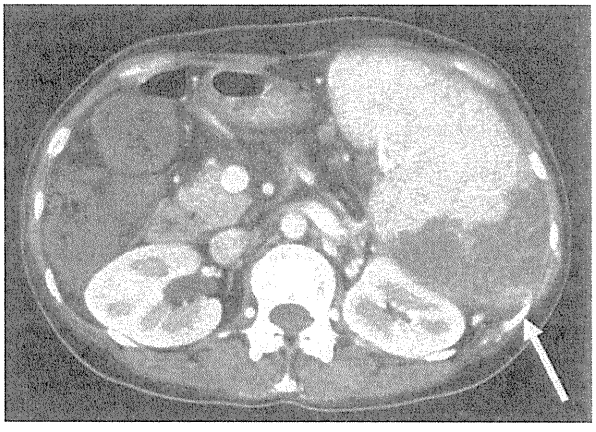

Fig. 2 Abdominal CT with contrast medium demonstrating partial splenic infarct demonstrated by a lack of contrast enhancement of the lower pole of the spleen (white arrow head)

また脾梗塞の病態としては，血液疾患や門脈圧亢進症では，脾臓の容積が増大するに従って相対的に脾臓実質の虚血が起こり，梗塞につながるとしている．実際 Nores ら[5]は 30 年間で 59 例の脾梗塞の症例の解析を行い，脾臓の平均重量は 1,180（90－4,975）g で，脾重量が 300 g を超えた症例が全体の 64% に，1,500 g を超えた症例が全体の 22% に認められたと報告している．本症例でも脾臓の重量は 1,120 g と巨脾であった．

胆汁うっ滞性肝硬変やその他の末期肝硬変患者に脾梗塞が発症した報告は少ないながらも散見される．Capron ら[6]は，脾梗塞を発症した 45 歳のアルコール性肝硬変の男性の患者を最初に報告している．患者は突然の左上腹部痛と高熱を訴え，腹腔動脈撮影で脾梗塞と診断された．梗塞範囲が大きかったため脾摘が行われた．摘出された脾臓の重量は 1,400 g で広い範囲に梗塞が認められた．また，Chin ら[7]は 3 例の脾梗塞患者を報告しているが，そのうち原発性硬化性胆管炎（PSC）の 22 歳女性は脾梗塞と診断された後，保存的に病状は改善したが，脾梗塞から 3 カ月後に脳死肝移植を受けている．他の 2 例の脾梗塞患者は，保存的治療により 4 週間で症状の改善した 23 歳の自己免疫肝炎の女性と保存的治療で症状がいったん改善したが，7 カ月後に同